Projective splines and estimators for planar curves

THOMAS LEWINER AND MARCOS CRAIZER

Departament of Matematics — Pontifícia Universidade Católica — Rio de Janeiro — Brazil
www.mat.puc--rio.br/~{tomlew,craizer}.

Abstract. Recognizing shapes in multiview imaging is still a challenging task, which usually relies on geometrical invariants estimations. However, very few geometric estimators that achieve projective invariance have been devised. This paper proposes a projective length and a projective curvature estimators for plane curves, when the curves are represented by points together with their tangent directions. In this context, the estimations can be performed with only three point-tangent samples for the projective length and five samples for the projective curvature. The proposed length and curvature estimator are based on projective splines built by fitting logarithmic spirals to the point-tangent samples. They are projective invariant and convergent.
Keywords: ***Projective Differential Geometry. Projective Splines. Projective Curvature. Projective Lenght. Discrete estimators.***

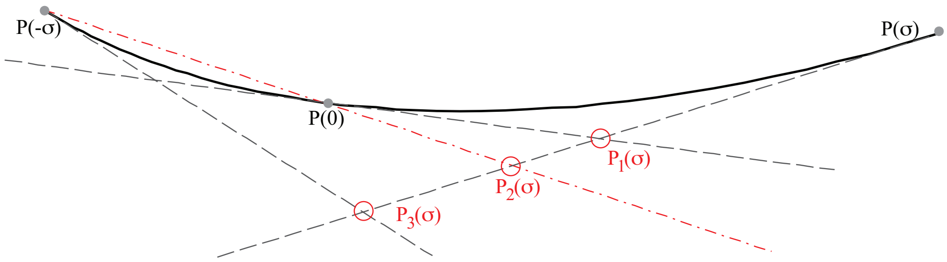

Figure 1: *Cross-ratio construction from point/tangent samples on the standard spiral.*

1 Introduction

Computer Vision applications usually deal with images that are two-dimensional projections of tridimensional scenes. Different projections of the same scene can be identified by isolating and matching the scene elements in each projection. This matching gets robust if it relies on quantities that are invariant by the projective group [18, 7, 2]. Projective length and projective curvature are the two simplest such quantities in differential geometry. Together, they are sufficient to describe a planar curve up to a projective transformation[6]. This means that a planar curve can be exactly identified in different projections such as photos, using those quantities, leading to a descriptor for curve matching, in the line of recent applications[16]. However, their estimation tends to be very sensitive to noise, since for a parametric curve, they depend on the fifth and seventh order derivatives respectively. This paper proposes numerically stable projective length and curvature estimators for planar curves.

Instead of considering discrete curves as a sequence of points, we choose here to sample a planar curve associating to each point its tangent direction. In Computer Vision, the curves of a scene are usually obtained by edge detection, which naturally generate these point-tangent samples. In this context, the projective length estimator uses only three point-tangent samples and the projective curvature estimator uses five of them. The same model was considered in [3, 4] to define affine length and affine curvature estimators.

The projective splines are obtained by fitting logarithmic spirals to the point-tangent samples. These spirals have projective curvature zero, similarly to polygonal lines in the Euclidean case [11] and parabolas in the affine case [3, 4]. The projective length of the spiral is estimated from a cross ratio of four points obtained from the data. The projective curvature estimator is obtained from the frames estimates at two consecutive samples. The proposed projective length and curvature estimators are proved to be convergent and numerical experiments included in this work show their numerical stability.

The work is an extension of [10], but the projective length estimator proposed here is much better: it is projective invariant. This fact makes the whole length and curvature estimations much more precise and efficient, as we can see by the experimental results. Moreover, with this new formulation, we could prove the convergence of both estimators.

Preprint MAT. 09/01, communicated on February 17^{th}, 2009 to the Department of Mathematics, Pontifícia Universidade Católica — Rio de Janeiro, Brazil. The corresponding work was published in Journal of Mathematical Imaging and Vision, Elsevier..

Related work. The study of analytic expression for projective curvature is laborious. Faugeras [6] describes very nicely the Euclidean, affine and projective geometry of plane curves, with explicit formulas for projective length and curvature. For affine quantities, the definition of affine invariants for discrete curves has been studied in several works. Callabi *et al.* [12, 13] propose affine length and curvature estimators with convergence proofs for curves given by a sequence of points, while Craizer *et al.* [3, 4] define estimators for curves given by points and tangent directions. These estimators are particular combinations of *joint invariants*, which are functions of the points' coordinates that are invariant under a given group action. Boutin [1] proposed joint invariants for Euclidean and affine groups. Olver [14] describes how to construct joint invariants for any group, in particular describing all joint invariants for the affine group in the plane. The authors of this work are not aware of any previous work that explicitly estimates projective lengths and curvatures for discrete curves. The probable reason for this absence is that these concepts deal with high order derivatives, which in general are numerically unstable. However, several works try to define projective quantities, in particular in multi-view images [17, 5, 9]. In particular, Lazebnik and Ponce [8] implement some notions of oriented projective geometry, introduced by Stolfi [15], to characterize silhouette features.

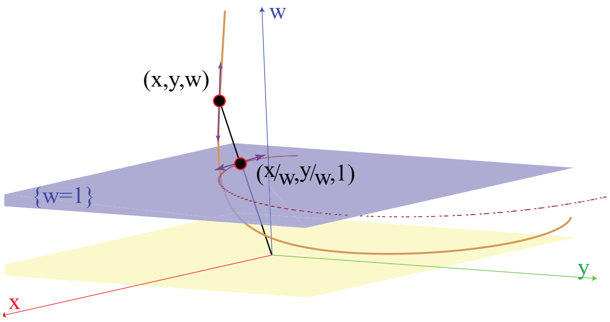

Figure 2: *Homogeneous coordinates on a logarithmic spiral: point $(\frac{x}{w}, \frac{y}{w}, 1)$ is the projection of point (x, y, w) onto the plane $\{w = 1\}$. They are projective equivalent points. Similarly, any line in the plane $\{\alpha \cdot (x, y, w) + \beta \cdot (x', y', 0)\}$ is projective equivalent to the tangent line at $(\frac{x}{w}, \frac{y}{w}, 1)$.*

2 Projective invariant geometry

In this section, we shall review the definitions of the basic quantities associated with smooth planar curves that are invariant under the projective group. We will denote a parametric curve C in homogeneous coordinates as $\mathbf{x}(t) = (x(t), y(t), w(t))$ (see Figure 2). The determinant of three vectors is denoted $|\mathbf{x}_1, \mathbf{x}_2, \mathbf{x}_3|$. With this notation, C is strictly convex if and only if $|\mathbf{x}''(t), \mathbf{x}'(t), \mathbf{x}(t)| \neq 0$ for any t.

In homogeneous coordinates, a projective transformation is defined by an invertible linear transformation of $\mathbb{R}^3$,

$$T = \begin{bmatrix} A & B & C \\ D & E & F \\ G & H & I \end{bmatrix},$$

taking into account that linear transformations T and λT are projective equivalent, for any $\lambda \neq 0$.

(a) Projective length and curvature.

Assuming that $|\mathbf{x}'', \mathbf{x}', \mathbf{x}| > 0$, we can decompose $\mathbf{x}'''$ on the frame $(\mathbf{x}, \mathbf{x}', \mathbf{x}'')$, obtaining: $\mathbf{x}''' + p\mathbf{x}'' + q\mathbf{x}' + r\mathbf{x} = 0$, where

$$p = -\frac{|\mathbf{x}''', \mathbf{x}', \mathbf{x}|}{|\mathbf{x}'', \mathbf{x}', \mathbf{x}|}, \quad q = \frac{|\mathbf{x}''', \mathbf{x}'', \mathbf{x}|}{|\mathbf{x}'', \mathbf{x}', \mathbf{x}|}, \quad r = -\frac{|\mathbf{x}''', \mathbf{x}'', \mathbf{x}'|}{|\mathbf{x}'', \mathbf{x}', \mathbf{x}|}.$$

Consider the function $H = r - \frac{1}{3}pq + \frac{2}{27}p^3 - \frac{1}{2}q' + \frac{1}{3}pp' + \frac{1}{6}p''$. Assuming that $H(t) \neq 0$, one defines the *projective length* σ by

$$\sigma(t) = \int_0^t \sqrt[3]{H(u)}du.$$

If one takes σ as a new parameter for the curve, then $H(\sigma) = 1$.

Since $\mathbf{x}(\sigma)$ and $\lambda(\sigma)\mathbf{x}(\sigma)$ are equivalent curves, we can force $p(\sigma)$ to be zero by choosing the value of $\lambda(\sigma)$ as $\lambda(\sigma) = \exp\left(\frac{1}{3}\int_0^\sigma p(\tau)d\tau\right)$ [6]. Thus,

$$\mathbf{x}'''(\sigma) + q(\sigma)\mathbf{x}'(\sigma) + r(\sigma)\mathbf{x}(\sigma) = 0. \tag{1}$$

Since $1 = H(\sigma) = r(\sigma) - \frac{1}{2}q'(\sigma)$, one can write $q(\sigma) = 2k(\sigma)$ and $r(\sigma) = k'(\sigma) + 1$. The number $k(\sigma)$ is called *projective curvature*.

We can write these equations as:

$$\begin{aligned} \frac{\partial \mathbf{x}}{\partial \sigma} &= \mathbf{x}_1 \\ \frac{\partial \mathbf{x}_1}{\partial \sigma} &= -k\mathbf{x} + \mathbf{x}_2 \\ \frac{\partial \mathbf{x}_2}{\partial \sigma} &= -\mathbf{x} - k\mathbf{x}_1 \end{aligned}$$

The frame $\{\mathbf{x}, \mathbf{x}_1, \mathbf{x}_2\}$ is called the *Frenet frame* of the curve.

(b) Curves of zero projective curvature.

In the normalized form of Equation (1), a zero projective curvature curve $\mathbf{x}(\sigma)$ satisfies the differential equation $\mathbf{x}'''(\sigma) + \mathbf{x}(\sigma) = 0$. A particular solution of this differential equation is the logarithmic spiral: $\mathbf{P}(\sigma) = (P_x(\sigma), P_y(\sigma), P_w(\sigma))$, with

$$\begin{cases} P_x(\sigma) = \mathbf{e}^{\frac{1}{2}\sigma}\cos\left(\frac{\sqrt{3}}{2}\sigma\right) \\ P_y(\sigma) = \mathbf{e}^{\frac{1}{2}\sigma}\sin\left(\frac{\sqrt{3}}{2}\sigma\right) \\ P_w(\sigma) = \mathbf{e}^{-\sigma} \end{cases}$$

Any other solution is given by $T \cdot \mathbf{P}(\sigma)$, where T is a projective transformation. The set of logarithmic spirals of zero projective curvature is thus an 8-dimensional vector space.

3 Projective splines: fitting spirals to data

In this paper, we consider the discretization of the curve C as a sequence $\{(\mathbf{x}_i, \mathbf{x}'_i)\}_{1\leq i\leq n}$ of point-tangent samples. We can think of $\mathbf{x}_i$ as a point $(x_i, y_i, 1)$ in the affine plane $z = 1$ and $\mathbf{x}'_i$ as a vector $(x'_i, y'_i, 0)$, parallel to $z = 1$ (see Figure 2). Moreover, $\mathbf{x}'_i$ indicates only the direction of the tangent to the curve, and its magnitude has no particular meaning.

Given three points-tangents samples, $(\mathbf{x}_{i-1}, \mathbf{x}'_{i-1})$, $(\mathbf{x}_i, \mathbf{x}'_i)$ and $(\mathbf{x}_{i+1}, \mathbf{x}'_{i+1})$, we want to fit a spiral with projective parameter 0 at $(\mathbf{x}_i, \mathbf{x}'_i)$, σ_i at $(\mathbf{x}_{i+1}, \mathbf{x}'_{i+1})$, and $-\sigma_i$ at $(\mathbf{x}_{i-1}, \mathbf{x}'_{i-1})$. Thus we have implicitly assumed that the projective lengths between samples are equal. We then deduce from the estimated spiral the frame $(\mathbf{Q}_i, \mathbf{Q}'_i, \mathbf{Q}''_i)$ at sample i.

(a) Relation between cross-ratio and projective length.

Consider the standard spiral $P(\sigma)$. For a fixed σ, let $P_1(\sigma)$ be the intersection of the tangent lines at $P(\sigma)$ and $P(0)$, $P_2(\sigma)$ be the intersection of the tangent line at $P(\sigma)$ and the line through $P(0)$ and $P(-\sigma)$, and $P_3(\sigma)$ be the intersection of the tangent lines at $P(\sigma)$ and $P(-\sigma)$ (see Figure 1).

We shall calculate the cross-ratio

$$f(\sigma) = [P(\sigma), P_1(\sigma), P_2(\sigma), P_3(\sigma)]\,.$$

Denote by $W = a\mathbf{e}^{a\sigma}$ the tangent vector of the spiral at $P(\sigma)$, with $a = \frac{3}{2} + \frac{i}{2}\sqrt{3}$. If we write $P_1 = P + uW$, $P_2 = P + vW$ and $P_3 = P + tW$, then the cross-ratio is given by

$$f(\sigma) = \frac{u(t-v)}{t(v-u)}.$$

But easy calculations show that

$$t = \frac{-\sqrt{3}\mathbf{e}^{-3\sigma} - 3\sin(\sqrt{3}\sigma) + \sqrt{3}\cos(\sqrt{3}\sigma)}{6\sin(\sqrt{3}\sigma)},$$

$$u = \frac{-\sqrt{3}\mathbf{e}^{-\frac{3\sigma}{2}} - 3\sin\left(\frac{\sqrt{3}\sigma}{2}\right) + \sqrt{3}\cos\left(\frac{\sqrt{3}\sigma}{2}\right)}{6\sin\left(\frac{\sqrt{3}\sigma}{2}\right)}$$

and

$$\begin{aligned} v \;=\; 2&\left[\mathbf{e}^{\frac{3\sigma}{2}}\sin\left(\frac{\sqrt{3}\sigma}{2}\right) + \mathbf{e}^{-\frac{3\sigma}{2}}\sin\left(\frac{\sqrt{3}\sigma}{2}\right) - \sin(\sqrt{3}\sigma)\right] \Big/ \\ &\left[-\mathbf{e}^{\frac{3\sigma}{2}}\left(3\sin\left(\frac{\sqrt{3}\sigma}{2}\right) + \sqrt{3}\cos\left(\frac{\sqrt{3}\sigma}{2}\right)\right) + \right. \\ &\left. 3\sin(\sqrt{3}\sigma) + \sqrt{3}\cos(\sqrt{3}\sigma)\right]\,. \end{aligned}$$

By making extensive but straightforward calculations, one can verify that $f(0) = 1$, $f'(0) = 0$, $f''(0) = 0$ and $f'''(0) = 6/5$. Thus f is an increasing function in a neighborhood of $\sigma = 0$. The graph of f is shown in Figure 3.

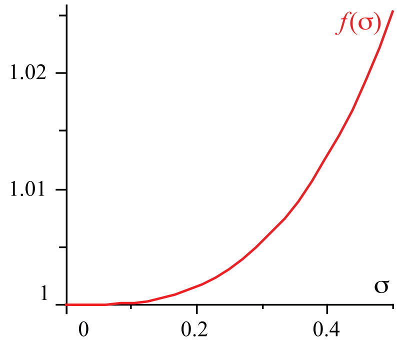

Figure 3: *The cross ratio function f from the projective length parameter σ.*

(b) Projective length estimator.

From the above paragraph, we can estimate the projective length σ_i between samples $\mathbf{x}_{i+1}$ and $\mathbf{x}_i$ (or $\mathbf{x}_i$ and $\mathbf{x}_{i-1}$). Denote by $\mathbf{x}_{i,1}$ the intersection of $\mathbf{x}'_{i+1}$ and $\mathbf{x}'_i$, by $\mathbf{x}_{i,2}$ the intersection of $\mathbf{x}'_{i+1}$ and the line through $\mathbf{x}_i$ and $\mathbf{x}_{i-1}$, and by $\mathbf{x}_{i,3}$ the intersection of $\mathbf{x}'_{i+1}$ and $\mathbf{x}'_{i-1}$. Then $\sigma_i = f^{-1}([\mathbf{x}_{i+1}, \mathbf{x}_{i,1}, \mathbf{x}_{i,2}, \mathbf{x}_{i,3}])$. We use a bisection algorithm to invert f. The projective length σ_i is in fact a convergent estimator as proved in the appendix.

(c) Linear equations of the fitting problem.

We know that there is a unique projective transformation $T_i = \left[\begin{smallmatrix} A & B & C \\ D & E & F \\ G & H & I \end{smallmatrix}\right]$ that takes $\mathbf{x}_{i-1}$ to $P(-\sigma_i)$, $\mathbf{x}_i$ to $P(0)$, $\mathbf{x}_{i+1}$ to $P(\sigma_i)$ and $\mathbf{x}_{i,3}$ to $P_3(\sigma_i)$.

The above conditions are described by the equations

$$\begin{aligned}
A\,P_x(0) + B\,P_y(0) + C &= (G\,P_x(0) + H\,P_y(0) + I)\cdot x_i \\
D\,P_x(0) + E\,P_y(0) + F &= (G\,P_x(0) + H\,P_y(0) + I)\cdot y_i \\
A\,P_x(\sigma_i) + B\,P_y(\sigma_i) + C &= (G\,P_x(\sigma_i) + H\,P_y(\sigma_i) + I)\cdot x_{i+1} \\
D\,P_x(\sigma_i) + E\,P_y(\sigma_i) + F &= (G\,P_x(\sigma_i) + H\,P_y(\sigma_i) + I)\cdot y_{i+1} \\
AP_x(-\sigma_i) + BP_y(-\sigma_i) + C &= (GP_x(-\sigma_i) + HP_y(-\sigma_i) + I)\cdot x_{i-1} \\
DP_x(-\sigma_i) + EP_y(-\sigma_i) + F &= (GP_x(-\sigma_i) + HP_y(-\sigma_i) + I)\cdot y_{i-1} \\
AP_{x,3}(\sigma_i) + BP_{y,3}(\sigma_i) + C &= (GP_{x,3}(\sigma_i) + HP_{y,3}(\sigma_i) + I)\cdot x_{i,3} \\
DP_{x,3}(\sigma_i) + EP_{y,3}(\sigma_i) + F &= (GP_{x,3}(\sigma_i) + HP_{y,3}(\sigma_i) + I)\cdot y_{i,3}
\end{aligned}$$

where we choose representatives of the points in the plane $w = 1$.

(d) Projective splines.

The spiral obtained by the above system defines an interpolation of the point/tangent samples in a projective invariant way. It has an explicit curve equation whose parameters are the coefficients of the projective transformation T_i and respects exactly the three points and tangents conditions. Moreover, these coefficients are continuous with respect to the three samples. Thus we may call it a *projective spline*.

(e) Estimating projective curvature

The estimated frame at sample i is given from the spiral's local frame: $(\mathbf{Q}_i, \mathbf{Q}'_i, \mathbf{Q}''_i) = T_i \cdot (\mathbf{P}, \mathbf{P}', \mathbf{P}'')$. It is clear that this frame estimator is projective invariant. In order to estimate the projective curvature, we need also an estimate of $\mathbf{Q}'''_i$ at sample i. Let

$$\mathbf{Q}'''_i = \frac{\mathbf{Q}''_{i+1} - \mathbf{Q}''_{i-1}}{2\sigma_i}. \tag{2}$$

The choice of central difference is justified in the next section. By decomposing the vector $\mathbf{Q}'''_i$ in the frame, one considers the coefficient k_i of $\mathbf{Q}'_i$ as the proposed projective curvature estimator. Thus, we have

$$k_i = \frac{|\mathbf{Q}'''_i, \mathbf{Q}''_i, \mathbf{Q}_i|}{4\sigma_i |\mathbf{Q}''_i, \mathbf{Q}'_i, \mathbf{Q}_i|}.$$

This projective curvature estimator is clearly projective invariant. The corresponding estimator for the integral of k, $\int k \, d\sigma$, is given by

$$\sum_{i=3}^{n-2} \frac{|\mathbf{Q}''_{i+1} - \mathbf{Q}''_{i-1}, \mathbf{Q}''_i, \mathbf{Q}_i|}{4|\mathbf{Q}''_i, \mathbf{Q}'_i, \mathbf{Q}_i|}. \tag{3}$$

This estimator is convergent as proved in the appendix.

4 Implementation and results

The implementation of the proposed estimators follows the description of the previous section. The cross ratio inversion for the length estimator is performed by a bisection method whose initial interval is centered on the affine-based length estimator of [10]. However, the fitting problem of section 3(c), although linear, should be handled with care. The curvature estimator then follows, but the convergence is much faster when using central finite differences, as described earlier. We have implemented these estimators to measure the estimation errors of discretized curves of known analytic length and curvature. The results confirm experimentally the convergence of the estimators proved in the appendix.

(a) Fitting problem inversion without division.

The fitting problem of section 3(c) is a homogeneous system with 8 equations and 9 unknowns (the coefficients of the transformation T_i). However, for small values of σ, the samples are almost aligned, and therefore the system is ill conditioned. We show here how to solve this system without division, overcoming this problem.

Grouping the equations in x and in y, it can be written as $S \cdot t = 0$ with

$$t = [A\,B\,C\,D\,E\,F\,G\,H\,I]^T$$

$$S = \begin{bmatrix} P & 0 & (-X \cdot P) \\ 0 & P & (-Y \cdot P) \end{bmatrix},$$

$$\text{where} \quad P = \begin{bmatrix} 1 & 0 & 1 \\ P_x(\sigma_i) & P_y(\sigma_i) & 1 \\ P_x(-\sigma_i) & P_y(-\sigma_i) & 1 \\ P_{x,3}(\sigma_i) & P_{y,3}(\sigma_i) & 1 \end{bmatrix},$$

$$\text{and} \quad \begin{array}{l} X = Diag\,(x_i, x_{i+1}, x_{i-1}, x_{i,3}) \\ Y = Diag\,(y_i, y_{i+1}, y_{i-1}, y_{i,3}) \end{array}.$$

This system can be solved directly as follows. Let $\tilde{P}$ be the squared matrix made of the first three lines of P:

$$\tilde{P} = \begin{bmatrix} 1 & 0 & 1 \\ P_x(\sigma_i) & P_y(\sigma_i) & 1 \\ P_x(-\sigma_i) & P_y(-\sigma_i) & 1 \end{bmatrix}.$$

Similarly let $\tilde{X}$ and $\tilde{Y}$ be the first three components of X and Y, respectively. We can invert $\tilde{P}$ to express unknowns A to F in function of G, H, I:

$$\begin{cases} \tilde{P}\,[A\,B\,C]^T &= \tilde{X}\tilde{P}\,[G\,H\,I]^T \quad , \\ \tilde{P}\,[D\,E\,F]^T &= \tilde{Y}\tilde{P}\,[G\,H\,I]^T \quad . \end{cases}$$

We are left with two homogeneous equations in G, H, I.

$$\begin{cases} V_G G + V_H H + V_I I = \left(P_3 \cdot \tilde{P}^{-1}\tilde{X}\tilde{P} - x_{i,3}P_3\right) \cdot [G\,H\,I]^T = 0 \\ W_G G + W_H H + W_I I = \left(P_3 \cdot \tilde{P}^{-1}\tilde{Y}\tilde{P} - y_{i,3}P_3\right) \cdot [G\,H\,I]^T = 0 \end{cases},$$

where P_3 is the last line of P: $P_3 = [P_{x,3}(\sigma_i)\; P_{y,3}(\sigma_i)\; 1]$. This incomplete homogeneous system can be solved by a simple cross product:

$$[G\,H\,I]^T = [V_G\,V_H\,V_I]^T \times [W_G\,W_H\,W_I]^T \quad .$$

In fact, a division is still present in the above homogeneous equations, when inverting $\tilde{P}$. Observe that $\det\left(\tilde{P}\right)$ vanishes when $\sigma_i = 0$. A straightforward Taylor expansion shows the flatness of this determinant near $\sigma_i = 0$:

$$\det\left(\tilde{P}\right) = \tfrac{3\sqrt{3}}{2}\sigma_i^3 + \tfrac{3\sqrt{3}}{4480}\sigma_i^9 + O(\sigma_i^{15}).$$

Since the system is homogeneous, we can consider the unknown to be $\sqrt[3]{\det(\tilde{P})}^{-1} t$ instead of t, or equivalently multiplying P by $\sqrt[3]{\det(\tilde{P})}$, leading to $\det(\tilde{P}) = 1$.

(b) Fast convergence with central finite difference.

The derivative $\mathbf{Q}'''_i$ in Equation (2) must be approximated with a discrete differentiation. The choice of forward or backward difference would have the advantage of requiring only four samples to compute the curvature and would simplify the expression of $\int k \, d\sigma$ in Equation (3). However, the convergence is slow, and central differences lead to much better accuracy of the estimators. This behavior can be observed in a simple case, where the input curve is the exact logarithmic spiral P around $\sigma = 0$. In this case, the projective transformation T_i is the identity matrix and the curvature vanishes: $k_i = 0$. We can compute the estimated curvature from Equation (2) explicitly:

$$\mathbf{Q}'''(0) = \begin{bmatrix} 1 \\ 0 \\ 1 \end{bmatrix}, \mathbf{Q}''(0) = \begin{bmatrix} -\frac{1}{2} \\ \frac{\sqrt{3}}{2} \\ 1 \end{bmatrix},$$

The corresponding work was published in Journal of Mathematical Imaging and Vision, Elsevier..

$$\text{and} \qquad \mathbf{Q}''(\sigma) = \begin{bmatrix} -\mathbf{e}^{\frac{1}{2}\sigma}\cos\left(\frac{\pi}{3} - \frac{\sqrt{3}}{2}\sigma\right) \\ \mathbf{e}^{\frac{1}{2}\sigma}\sin\left(\frac{\pi}{3} - \frac{\sqrt{3}}{2}\sigma\right) \\ \mathbf{e}^{-\sigma} \end{bmatrix}.$$

A straightforward Taylor expansion shows that

$$\begin{aligned} k_i^{forward} &= \frac{|\mathbf{Q}''_{i+1} - \mathbf{Q}''_i, \mathbf{Q}''_i, \mathbf{Q}_i|}{2\sigma_i|\mathbf{Q}''_i, \mathbf{Q}'_i, \mathbf{Q}_i|} \\ &= \tfrac{1}{2}\sigma_i - \tfrac{1}{240}{\sigma_i}^4 + O({\sigma_i}^7), \\ k_i^{central} &= \frac{|\mathbf{Q}''_{i+1} - \mathbf{Q}''_{i-1}, \mathbf{Q}''_i, \mathbf{Q}_i|}{4\sigma_i|\mathbf{Q}''_i, \mathbf{Q}'_i, \mathbf{Q}_i|} \\ &= -\tfrac{1}{240}{\sigma_i}^4 + O({\sigma_i}^{10}). \end{aligned}$$

Thus, for small values of σ_i, the estimator $k_i^{central}$ is much more precise.

(c) Numerical experiments.

In our model, as in several discrete models [11], curvature is concentrated at vertices. Therefore, the convergence can be better observed on integrals of the curvature rather than on punctual curvature. The same is true for the length. We therefore compared our estimators with analytic ones by computing $\int d\sigma$ and $\int k\ d\sigma$ (Equation (3)). In order to compare our estimators with the analytical length and curvature integrals, we restricted our experiments to spirals and power curves, where we could explicitly compute these invariants. To check the convergence for denser samplings, i.e. small σ_i, we used a multi-precision library (`MPFR C++`).

The convergence of both estimators can be observed on Figure 4. However, when the sampling is not regular, as for the power curve sampled as $(t^n, t^m, 1)$, the convergence is much slower than when sampled uniformly (see Figures 5 and 6). The estimator in multi-precision needs around 4 milliseconds per point on a 2.8GHz computer, and only fractions of millisecond in standard double precision.

The estimators are projective invariant, since the algorithm deals only with projective quantities. To illustrate this numerically, we consider the same curves before and after projective transformations (see Figure 7). To get an order of the sampling density, these examples are for curves with 50 samples (the sparsest sampling on Figures 5 and 6), which would correspond to an average distance of 10 to 15 pixels between sample, if the curve fits on a 1024×768 image.

5 Conclusion and future works

In this paper, estimators for the projective length and curvature of a plane curve given by point-tangent samples are proposed. The projective estimators are based on an estimator of the frame at each sample, which is obtained by fitting logarithmic spirals to the given data. Its convergence is proved and verified in numerical experiments.

Since the differential definitions of the projective length and curvature involve seventh order derivatives, robustness is a very delicate issue. The presence of noise may thus have a significative impact on the result, particularly for noise affecting the tangent sample. Moreover, the hypothesis of regular sampling for the projective spline fitting may not be respected, which harms the stability of the method (e.g. comparing Figures 5 and 6), although still ensuring projective invariance. However, the design of the solution without division and the analysis of the right finite difference scheme turns the method robust to degenerate case such as almost aligned samples.

As future work we propose to consider tridimensional surfaces defined by points and tangent planes. In this context, one can try to define Euclidean, affine or projective estimators.

Acknowledgements

The authors would like to thank CNPq and FAPERJ for their financial support during the preparation of this work.

References

[1] M. Boutin. Numerically invariant signature curves. *International Journal of Computer Vision*, 40(3):235–248, 2000.

[2] M. Boutin. On invariants of Lie groups and their application to some equivalence problems. PhD thesis, *University of Minnesota*, 2001.

[3] M. Craizer, T. Lewiner and J.-M. Morvan. Parabolic polygons and discrete affine geometry. In *Sibgrapi*, pages 11–18. IEEE, 2006.

[4] M. Craizer, T. Lewiner and J.-M. Morvan. Combining points and tangents into parabolic polygons: an affine invariant model for plane curves. *Journal of Mathematical Imaging and Vision*, 29(2-3):131–140, 2007.

[5] R. Fabbri and B. Kimia. High-Order Differential geometry of Curves for Multiview Reconstruction and Matching. In *Energy Minimization Methods in Computer Vision and Pattern Recognition*, pages 645–660. Springer, 2005.

[6] O. Faugeras. Cartan's moving frame method and its application to the geometry and evolution of curves in the Euclidean, affine and projective planes. In *Workshop on Applications of Invariance in Computer Vision*, pages 11–46. Springer, 1994.

[7] C. E. Hann. Recognizing two planar objects under a projective transformation. PhD thesis, *University of Canterbury*, 2001.

[8] S. Lazebnik and J. Ponce. The Local Projective Shape of Smooth Surfaces and Their Outlines. *International Journal of Computer Vision*, 63(1):65–83, 2005.

[9] S. Lazebnik, Y. Furukawa and J. Ponce. Projective Visual Hulls. *International Journal of Computer Vision*, 74(2):137–165, 2007.

[10] T. Lewiner and M. Craizer. Projective estimators for point-tangent representations of planar curves. In *Sibgrapi*, pages 223–229, 2008.

[11] F. Mokhtarian and A. K. Mackworth. A theory for multiscale, curvature based shape representation for planar curves. *IEEE Transactions on Pattern Analysis and Machine Intelligence*, 14:789–805, 1992.

[12] E. Calabi, P. J. Olver and A. Tannenbaum. Affine geometry, curve flows, and invariant numerical approximations. *Advances in Mathematics*, 124:154–196, 1997.

[13] E. Calabi, P. J. Olver, C. Shakiban, A. Tannenbaum and S. Hacker. Differential and numerically invariant signature curves applied to object recognition. *International Journal of Computer Vision*, 26(2):107–135, 1998.

[14] P. J. Olver. Joint invariant signatures. *Foundations of Computational Mathematics*, 1(1):3–67, 2001.

[15] J. Stolfi. *Oriented projective geometry*. Academic Press, Boston, 1991.

[16] F. M. Sukno, J. J. Guerrero and A. F. Frangi. Projective active shape models for pose-variant image analysis of quasi-planar objects: Application to facial analysis. *Pattern Recognition*, 2009. to appear.

[17] B. Triggs. Camera Pose and Calibration from 4 or 5 known 3D Points. In *International Conference on Computer Vision*, pages 278–284, 1999.

[18] C. Rothwell, A. Zisserman, D. Forsyth and J.L.Mundy. Planar object recognition using projective shape representation. *International Journal of Computer Vision*, 16(1):57–99, 1995.

A Convergence of the estimators

To make calculations easier, we use complex notation in this appendix. Consider a smooth curve $\mathbf{w}(t)$ and the standard spiral $\mathbf{z}(\sigma) = \mathbf{e}^{a\sigma}$, where $a = \frac{3}{2} + i\frac{\sqrt{3}}{2}$. Assume that the three point-tangent samples at $\mathbf{w}(t_2)$,$\mathbf{w}(0)$ and $\mathbf{w}(t_1)$, $t_2 < 0$, $t_1 > 0$ are fitted by the standard spiral at $-\sigma_1$, 0 and σ_1, which writes

$$\begin{cases} \mathbf{w}\,(t_1) &= & \mathbf{z}(\ \ \sigma_1) & , \\ \mathbf{w}\,(t_2) &= & \mathbf{z}(-\sigma_1) & , \\ \mathbf{w}'(t_1) &\parallel & \mathbf{z}'(\ \ \sigma_1) & , \\ \mathbf{w}'(t_2) &\parallel & \mathbf{z}'(-\sigma_1) & . \end{cases} \tag{4}$$

Any such smooth curve that passes through $z(0)$ and has tangent line parallel to $z'(0)$ can be written as $\mathbf{w}(t) = \mathbf{e}^{a(t+b(t)t^2}$. We first reduce the problem to the case where $b(t)$ is purely imaginary.

Claim 1: By a change of variables, we can assume that $b(t) = i\beta(t)$, with $\beta(t)$ real.
In fact, if $b(t) = \beta_1(t) + i\beta_2(t)$, we consider $u = t + \beta_1(t)t^2$ to obtain $\mathbf{w}(u) = \mathbf{e}^{a(u+i\beta(u)u^2}$.

The second claim shows that $\beta(t)$ is close to 0 in the C^3 topology if the sampling is dense enough.
Claim 2: We have that $t_1 = -t_2 = \sigma_1$ and we can write $\beta(t) = \gamma(t)(t^2 - t_1^2)^2$.

In fact, we can rewrite Equation (4) as

$$\begin{cases} t_1 + i\beta(t_1)t_1^2 &= & \sigma_1 \\ t_2 + i\beta(t_2)t_2^2 &= & -\sigma_1 \\ 2t_1\beta(t_1) + \beta'(t_1)t_1^2 &= & 0 \\ 2t_2\beta(t_2) + \beta'(t_2)t_2^2 &= & 0 \end{cases}$$

We conclude that $t_1 = -t_2 = \sigma_1$ and that $\beta(t_1) = \beta'(t_1) = \beta(t_2) = \beta'(t_2) = 0$.

Denote by s the projective lengths of $\mathbf{w}$ in the interval $[t_2, t_1]$. We have computed this projective length with a symbolic calculation software and obtained that

$$s = 2t_1 + O(t_1^3),$$

thus proving the convergence of the projective length estimator.

Denote by (w_i, w_i', w_i'') the Frenet frame of $\mathbf{w}$ at $\mathbf{x}_i$, and by (Q_i, Q_i', Q_i'') the estimated Frenet frame: Observe that $Q_i = w_i = w(0) = 1$, $Q_i' = w_i' = w'(0) = a$ and $w_i'' = w''(0) = a^2 + 2a\beta(0)i$. Since $Q_i'' = a^2$, we conclude that $Q_i'' = w_i'' + O(t_i^4)$. From this, it easy to prove the convergence of the projective curvature estimator.

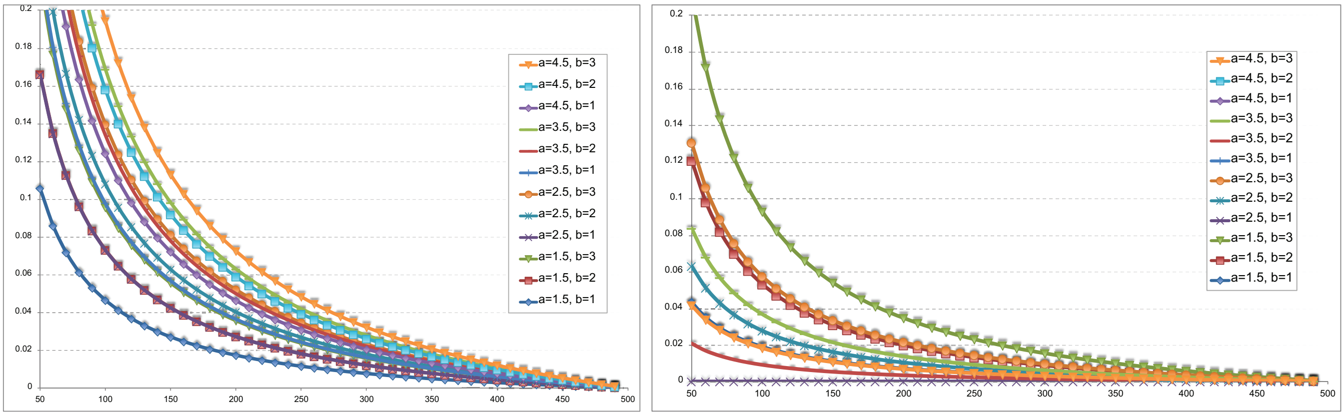

Figure 4: *Convergence tests on logarithmic spirals* $(e^{a\cdot t}\cos((b+\sqrt{3}/2)t), e^{a\cdot t}\sin((b+\sqrt{3}/2)t), e^{-t})$, $t \in [0.1, 1.1]$ *uniformly sampled: number of samples* $\times$ *error of the estimators* $\int d\sigma$ *(left) and* $\int k\, d\sigma$ *(right) compared with the analytical quantities.*

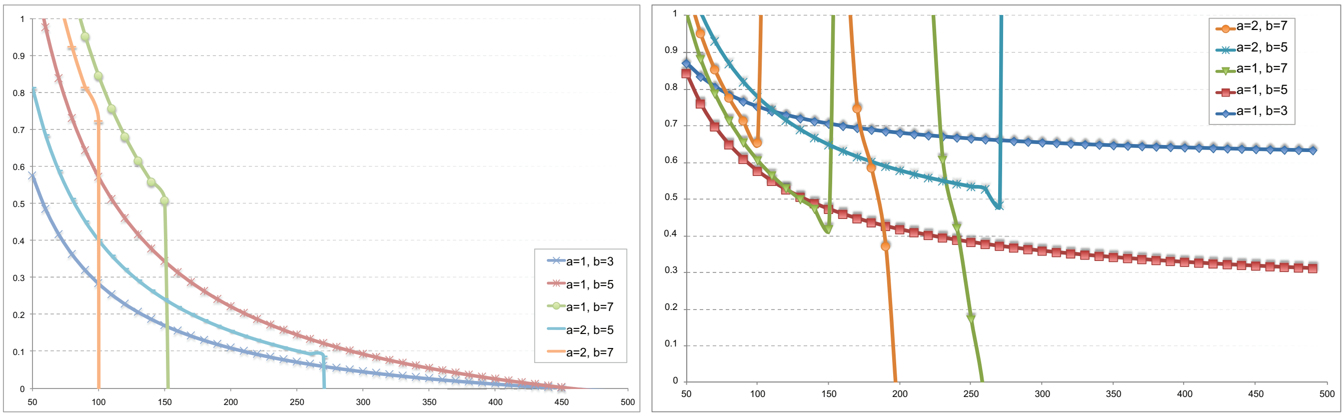

Figure 5: *Convergence test on power curves* $(t^a, t^b, 1)$, $t \in [0.1, 1.1]$, *sampled regularly in* t*: number of samples* $\times$ *error of the estimators* $\int d\sigma$ *(left) and* $\int k\, d\sigma$ *(right) compared with the analytical quantities. The sharp variations of the projective length between samples close to* $t = 0.1$ *harms the convergence of the estimators.*

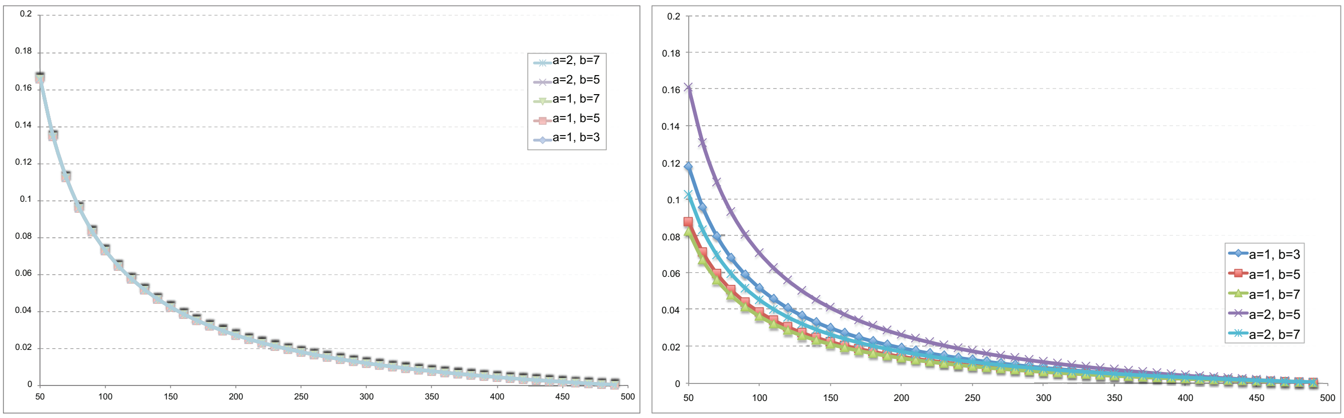

Figure 6: *Convergence test on power curves* $(t^a, t^b, 1)$, $t \in [0.1, 1.1]$, *uniformly sampled in* σ*: number of samples* $\times$ *error of the estimators* $\int d\sigma$ *(left) and* $\int k\, d\sigma$ *(right) compared with the analytical quantities. As opposed to the tests of Figure 5, the uniform sampling ensures the convergence of the estimators.*

Preprint MAT. 09/01, communicated on February 17^{th}, 2009 to the Department of Mathematics, Pontifícia Universidade Católica — Rio de Janeiro, Brazil.

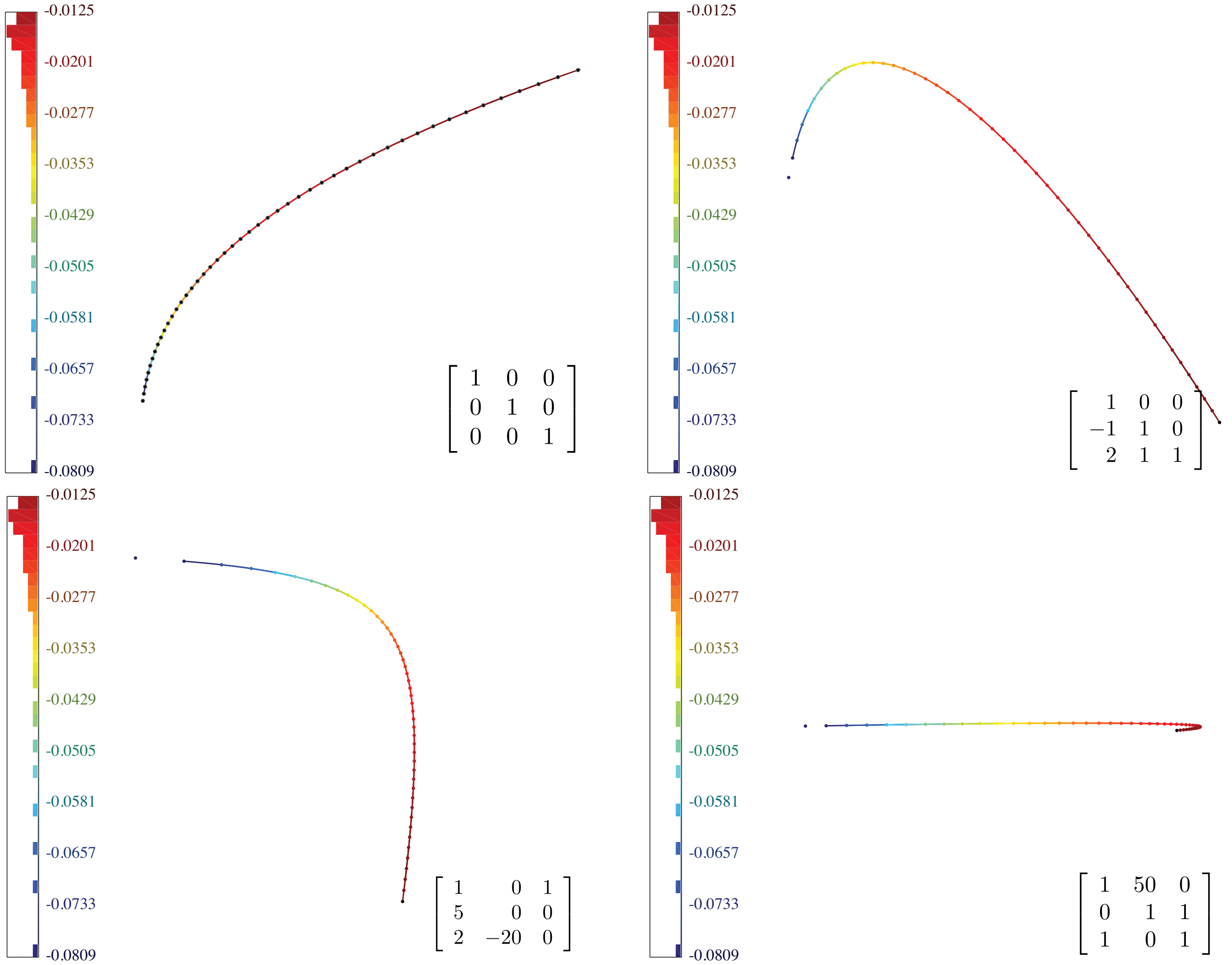

Figure 7: *The estimated projective length on a polynomial curve* $(t^2\sqrt{t}, t, 1)$ *sampled with 50 points ant tangent, regularly in t, i.e. not equally spaced. Comparing before (top) and after (subsequent) projection illustrate the projective invariance of the estimator.*

The corresponding work was published in Journal of Mathematical Imaging and Vision, Elsevier..